Direct Calculation of Thermodynamic Wet-Bulb Temperature as a Function of Pressure and Elevation

SAYED-HOSSEIN SADEGHI AND TROY R. PETERS

Washington State University, Prosser, Washington

DOUGLAS R. COBOS

Decagon Devices, Pullman, Washington

HENRY W. LOESCHER

National Ecological Observatory Network, and Institute of Arctic and Alpine Research, University of Colorado, Boulder, Colorado

COLIN S. CAMPBELL

Decagon Devices, Pullman, Washington

(Manuscript received 6 September 2012, in final form 29 January 2013)

ABSTRACT

A simple analytical method was developed for directly calculating the thermodynamic wet-bulb temperature from air temperature and the vapor pressure (or relative humidity) at elevations up to 4500 m above MSL was developed. This methodology was based on the fact that the wet-bulb temperature can be closely approximated by a second-order polynomial in both the positive and negative ranges in ambient air temperature. The method in this study builds upon this understanding and provides results for the negative range of air temperatures (−17° to 0°C), so that the maximum observed error in this area is equal to or smaller than −0.17°C. For temperatures ≥0°C, wet-bulb temperature accuracy was ±0.65°C, and larger errors corresponded to very high temperatures ($T_a \geq 39$°C) and/or very high or low relative humidities (5% < RH < 10% or RH > 98%). The mean absolute error and the root-mean-square error were 0.15° and 0.2°C, respectively.

1. Introduction

First principles dictate that for any given ambient air mass, the difference between aspirated (well coupled) air temperature that includes ambient water vapor (dry-bulb temperature T_a) and the temperature of the same air mass (wet-bulb temperature T_w) at saturation provides a direct measurement of the amount of water vapor that air mass contains. This estimate can be determined as both relative and absolute quantities (Loescher et al. 2009). In other words, T_w is the temperature that a volume of air would have if cooled adiabatically to saturation at a constant pressure where all the heat energy came from the measured volume of air (Monteith 1965). The importance of this first principle is better realized when the T_a and T_w measured at both a surface level (boundary condition) and at different heights, that is, reference levels, can be used to estimate the evapotranspiration vertically through these two levels, for example, through a leaf or a canopy surface (Slatyer and McIlroy 1961; Alves et al. 2000; Balogun et al. 2002a,b).

Wet-bulb temperature is a basic hydrostatic, physical quantity that can be used to estimate basic physical weather parameters (Stull 2011). Some applied applications of T_w include linking surface and boundary layer flows (Wai and Smith 1998) and interpreting surface scalar fluxes using physical properties (Loescher et al. 2006), while practical applications may be determining the efficiency of industrial coolers (Gan and Riffat 1999), managing hydrological resources (Dunin and Greenwood

Corresponding author address: Troy Peters, Washington State University, 24106 N. Bunn Rd., Prosser, WA 99350.
E-mail: troy_peters@wsu.edu

DOI: 10.1175/JTECH-D-12-00191.1

1986), and identifying saturated adiabats on thermodynamic isopleths (Stull 2000).

Another commonplace and important application of T_w is in agricultural research and management, and its determination has important implications on agronomic economies. For instance, T_w is used to determine (i) the amount of time and energy required to dry grain to a stable storage moisture content (Schmidt and Waite 1962), (ii) frost protection for fruit crops (e.g., G. Hoogenboom 2012, personal communication), and (iii) minimum temperature forecasts on relatively clear nights (Angström 1920, abstracted in Smith 1920).

The determination of the theoretical thermodynamic wet-bulb temperature can be solved by the following equation (ASABE 2006):

$$e_s(T_w) - e_a = B(T_w - T_a), \tag{1}$$

where e_a is the ambient vapor pressure (kPa), T_a is the dry-bulb temperature (K), $e_s(T_w)$ is the saturated vapor pressure at T_w (kPa), and B is the thermodynamic psychometric constant given by

$$B = \frac{m[e_s(T_w) - P_a]\left(1 + n\dfrac{e_a}{P_a}\right)}{qh_{\mathrm{fg}}}. \tag{2}$$

In Eq. (2), m, n, and q are empirical coefficients; P_a is the atmospheric pressure head (kPa); and h_{fg} is the latent heat of vaporization of water at T_w (J kg^{-1}) defined by Brooker (1967) and where

$$h_{\mathrm{fg}} = r - s(T_w - 273.16). \tag{3a}$$

Both r and s are empirically determined coefficients. Equation (3a) is valid when $0° \le T_w \le 65.6$°C. For negative values of T_w ($-17.8° \le T_w \le 0$°C), h_{fg} in Eq. (2) must be replaced by the latent heat of sublimation (h_{ig}) at T_w (Brooker 1967), such that

$$h_{\mathrm{ig}} = t - u(T_w - 255.38), \tag{3b}$$

where both r and s are empirically determined coefficients. Also, P_a can be determined as (Campbell and Norman 1998)

$$P_a = 101.3 \exp\left(\frac{-H}{8200}\right), \tag{3c}$$

with H being the elevation (m).

If we assume that the thermodynamic wet-bulb temperature [from Eq. (1)] and the wet-bulb temperature T_w^* (empirical, measured by a thermometer) are approximately the same, then Eq. (1) takes the following form:

$$e_a - e_s(T_w^*) + \gamma P_a(T_a - T_w^*) = 0, \tag{4}$$

where γ is the psychometric constant (°C^{-1}) defined by $\gamma = C_p/L_v \approx 0.4[\mathrm{g_{water}}\ (\mathrm{kg_{air}})^{-1}\ \mathrm{K}^{-1}]$ (where C_p is the specific heat of moist air at constant pressure and L_v is the latent heat of vaporization). The historical approach of using B in Eq. (1) converts the temperature depression into vapor pressure deficit through the estimation of empirical coefficients and empirical quantification of the latent energy. Substituting γP_a for B in Eq. (4) takes the same form of unit conversion but removes the uncertainty from the empirical coefficients.

Because Eq. (1) [or Eq. (4)] has no direct solution for T_w (or T_w^*), typically a trial-and-error process is carried out to find an accurate estimation. Using computers, this requires considerable amounts of CPU time to analyze large weather databases. Alternatively, one can employ a graphical solution by through the use psychrometric diagrams (ASHRAE 1997). This latter method, however, has large associated uncertainties because of human errors (Brooker 1967) and must use a priori, predetermined curve fits for each value of the atmospheric pressure.

Noniterative and analytical approaches have been suggested to calculate T_w. Sreekanth et al. (1998) used artificial neural networks that require relative humidity (RH) and the dewpoint temperature (T_d) estimates as input variables. Chappell et al. (1974) calculated T_w by estimating the amount of dry air needed to dry a given mass of moist air through an isobaric and adiabatic procedure, and they reported an accuracy of ±1°C across ambient ranges of atmospheric temperature and pressure when wet-bulb depressions were <30°C. Chau (1980) presented empirical equations to find the T_w by dividing the psychrometric chart into seven arbitrary ranges that span T_a values of −32° to 260°C and T_d values of −32° to 40°C, but found this technique only to be accurate (and valid) at sea level.

The crux of all of the above-mentioned solutions requires known T_d temperatures to derive T_w. Alternatively, some studies have combined estimates of T_a and RH with either a third-order polynomial equation for $e_s(T_w^*)$ [as in the case with Tejeda-Martínez (1994)] or with gene-expression programming (i.e., Stull 2000) to derive the wet-bulb temperature. Both studies found this methodology was not valid for ambient conditions with low values of T_a (i.e., <10°C), and/or with low values of RH (i.e., Stull 2000). The Stull (2000) methodology was also only valid at sea level.

Additional uncertainties are the result in the choice of which value of the psychrometric constant is used, particularly when (i) a constant value is chosen [e.g., 6.53×10^{-4} °C^{-1} (Tejeda-Martínez 1994), 6.67×10^{-4} (Schurer 1981), and 5.68×10^{-4} °C^{-1} to 6.42×10^{-4} °C^{-1} when

$T_w \leq 0°$ and $0° < T_w < 30°C$ (Simões-Moreira 1999)] and (ii) theoretical estimations of γ outlined in Eq. (1) are being questioned empirically (Simões-Moreira 1999; Loescher et al. 2009). As such, these studies have empirically shown that γ is independent of T_a and P_a (Simões-Moreira 1999; Loescher et al. 2009), and they have demonstrated its value is strongly dependent on T_w (Simôes-Moreira 1999) and the wet-bulb depression (Loescher et al. 2009).

The objective of this study is to derive a direct solution for calculating the T_w at any desired elevation while maintaining the high levels of accuracy needed for most applications. This will be achieved by first finding a direct solution for calculating T_w^* from Eq. (4) and then exploring its mathematical derivations to enhance the accuracy in T_w estimates.

2. Methodology

Mathematical derivations

In this study, we are interested in the range of T_a used for most basic and applied research ($-17°C \leq T_a \leq 40°C$) and assumed the Simões-Moreira's (1999) values for γ are accurate. The saturated vapor pressure in Eq. (4) is estimated by the Magnus equation (Murray 1967):

$$e_s(T_a) = \alpha \exp\left(\frac{bT_a}{T_a + c}\right), \tag{5a}$$

$$e_s(T_w^*) = \alpha \exp\left(\frac{bT_w^*}{T_w^* + c}\right), \tag{5b}$$

where a, b, and c are empirical coefficients that depend on the interval by which temperature is being measured (Table 1). Buck (1981) reported that Eq. (5a) led to a maximum 5%–6% deviation from ''truth'' and resulted in a positive divergence (when conditions were $0° \leq T_a \leq 50°C$) and negative divergence (when conditions were $-40° \leq T_a \leq 0°C$), when compared with the Wexler (1976) derivation of $e_s(T_a)$. Similarly, $e_s(T_w^*)$ can be estimated by Eq. (5b). Substitution of P_a from Eq. (3c) and $e_s(T_w^*)$ from Eq. (5b) into Eq. (4) results in

$$a \exp\left(\frac{bT_w^*}{T_w^* + c}\right) - e_a - 101.3\gamma \exp\left(\frac{-H}{8200}\right)(T_a - T_w^*) = 0. \tag{6}$$

To find a solution to estimate T_w^* [Eq. (6)], we numerically applied different combinations of T_w^*, T_a, e_a, and H. In each combination, T_a, H, and e_a were held constant and only T_w^* was altered. We used two discrete

TABLE 1. Coefficients for calculating saturated vapor pressure of pure water as a function of temperature after Buck (1981).

Temp interval (°C)	a	b	c
0 to 50	0.611	17.368	238.88
−40 to 0	0.611	17.966	247.15

T_w^* ranges, that is, $-30° \leq T_w^* < 0°C$ and $0° \leq T_w^* \leq 40°C$, and in preliminary analyses, Eq. (6) closely followed the shape of a second-order polynomial (Fig. 1). Not surprisingly, this relationship was more curvilinear for positive T_a values. Note that the intersection of each curve with the horizontal axis represents T_w^*. Based on this, an equivalent form for Eq. (6) can heuristically be considered as

$$a \exp\left(\frac{bT_w^*}{T_w^* + c}\right) - e_a - 101.3\gamma \exp\left(\frac{-H}{8200}\right)(T_a - T_w^*) \cong \lambda(T_w^*)^2 + \phi T_w^* + \psi = 0, \tag{7}$$

where λ, φ, and ψ are empirical coefficients, and the advantage of using Eq. (7) can be rearranged to explicitly calculate T_w^* as

$$T_w^* \cong \frac{-\varphi + \sqrt{\Delta}}{2\lambda}, \tag{8a}$$

where

$$\Delta = \phi^2 - 4\lambda\psi. \tag{8b}$$

It is worth noting that Eq. (7) is inherently an ascendant function (the derivative at any arbitrary point is always positive), making an acceptable value of T_w^* always the larger root of the second-order polynomial (i.e., Figs. 1a–h) and therefore, the positive sign should always be inserted before $\sqrt{\Delta}$ in Eq. (8a).

Because the solutions for λ, φ, and ψ are infinite given any suite of environmental conditions [Eq. (7)], we evaluated them at three different logical conditions of T_w^*. For the positive T_w^* region ($0° \leq T_w^* \leq 40°C$), these fixed conditions were $T_w^* = 0$, $T_w^* = T_a/2$, and $T_w^* = T_a$. This is a logical selection because T_w^* is always $\leq T_a$, and in other words, the ambient T_a is the last value to be substituted into Eq. (7). For negative values ($-17° \leq T_w^* < 0°C$), the selection of $T_w^* = T_a$ could not be addressed mathematically because values of T_w are always $< T_a$ and do not necessarily cover the whole negative range of Eq. (7). Applying the logic from Stull (2000, his Fig. 1), the wet-bulb depressions ($T_a - T_w^*$) did not exceed 6°C when T_w^* was negative and when the RH was >20%.

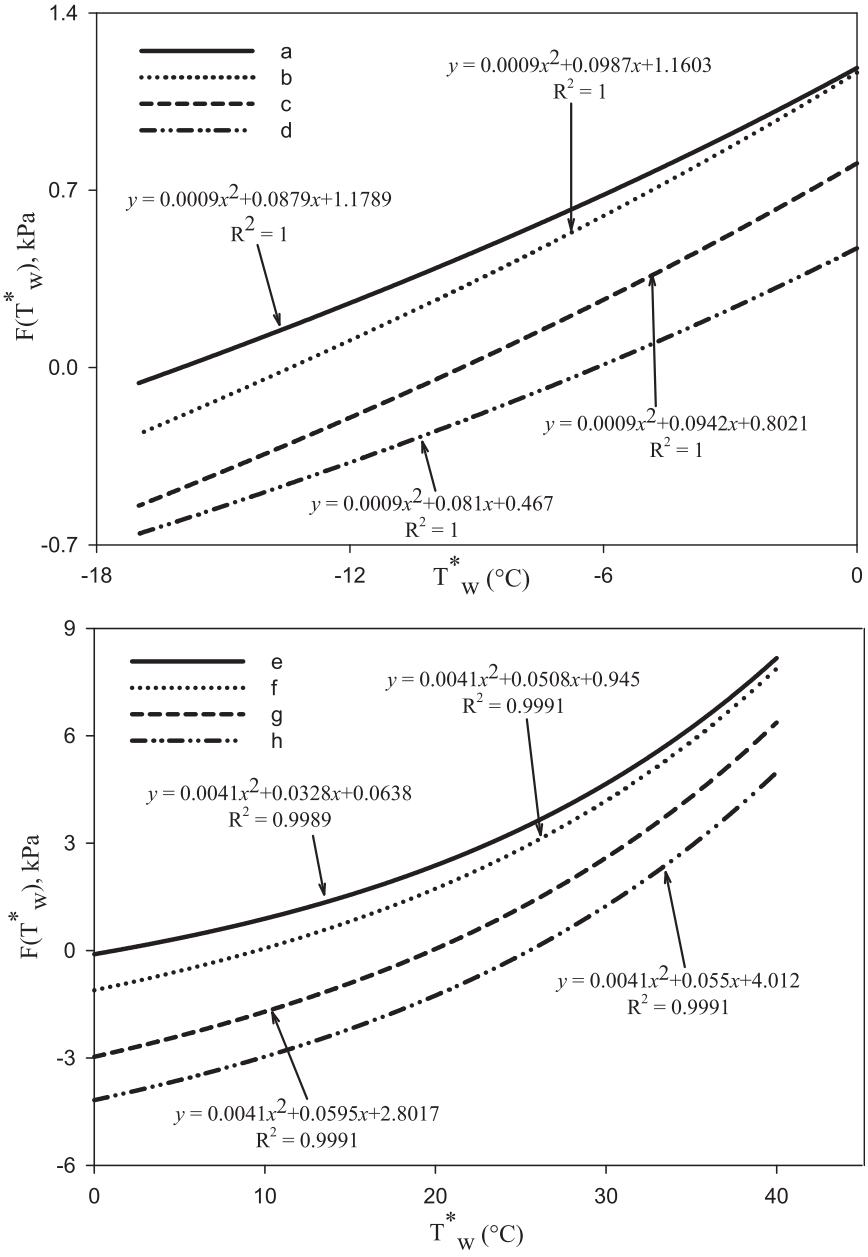

FIG. 1. Variation of $F(T_w^*)$ in Eq. (6) with (top) negative range of the wet bulb where for line a, $H = 1700$ m, $e_a = 0.13$ kPa, and $T_a = -15$°C; line b, $H = 0$ m, $e_a = 0.08$ kPa, and $T_a = -11$°C; line c, $H = 660$ m, $e_a = 0.23$ kPa, and $T_a = -8$°C; and line d, $H = 3000$ m, $e_a = 0.3$ kPa, and $T_a = -4$°C; and (bottom) positive range of the wet bulb where line e, $H = 4500$ m, $e_a = 0.6$ kPa, and $T_a = 3$°C; line f, $H = 1300$ m, $e_a = 1$ kPa, and $T_a = 13$°C; line g, $H = 100$ m, $e_a = 3$ kPa, and $T_a = 9$°C; and line h, $H = 700$ m, $e_a = 2.4$ kPa, and $T_a = 40$°C.

This similarity of T_a and T_w^* provides the rationale to use the same set of fixed conditions when T_w^* is negative as when T_w^* is positive. Thus, the mathematical derivations yielded

$$\psi = a - \gamma P_a T_a - e_a, \tag{9a}$$

$$\lambda = \frac{2a\left[\exp\left(\frac{bT_a}{T_a + c}\right) - 2\exp\left(\frac{bT_a}{T_a + 2c}\right) + 1\right]}{T_a^2}, \tag{9b}$$

$$\phi = \zeta(T_a) + \gamma P_a, \tag{9c}$$

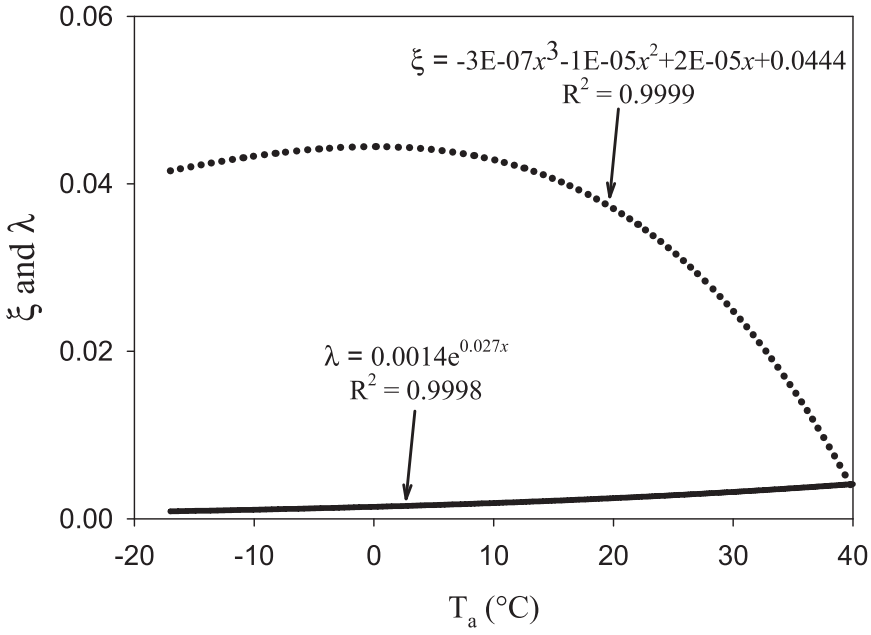

FIG. 2. Relationship between λ (black line) and ζ (dotted line) as a function of temperature when $-17° \le T_a \le 40°C$, $\lambda = 0.0014 \exp(0.027T_a)$ with $R^2 = 0.9998$, and $\zeta = -[3 \times 10^{-07}(T_a)^3] - [1 \times 10^{-05}(T_a)^2] + [2 \times 10^{-05}(T_a)] + 0.0444$ with $R^2 = 0.9999$. Note that T_a in the denominator of the λ function has the exponent 2 [Eq. (9b)], whereas its exponent value in ζ is 1 [Eq. (10)], making the shapes of the two functions quite different. Hence, we choose different regression equations.

where the function ξ is given by

$$\zeta = \frac{4a \exp\left(\frac{bT_a}{T_a + 2c}\right) - a \exp\left(\frac{bT_a}{T_a + c}\right) - 3a}{T_a}. \quad (10)$$

To determine the dependency of T_a on λ and ξ, a series of numerical operations were again carried out. For this purpose, the values of T_a were varied from $-17°$ to 40°C by an increment of 0.1°C (Fig. 2). For both parameters, the statistical relationships were nonlinear, as presented below and described in the Fig. 2 caption. The proposed analytical solution therefore includes the derivation of λ and ξ from these statistical relationships, calculating ψ and φ by Eqs. (9a) and (9c), and finally T_w^* by Eq. (8a), where

$$\lambda = 0.0014e^{0.027T_a}, \quad (11)$$

$$\zeta = (-3 \times 10^{-7})T_a^3 - (10^{-5})T_a^2 + (2 \times 10^{-5})T_a + 4.44 \times 10^{-2}. \quad (12)$$

3. Results

Validation

The accuracy of the analytical solution derived here for calculating T_w^* was tested by comparing it with the solution found in Eq. (1). For this purpose, a series of numerical, iterative computations were carried out to calculate a highly accurate and theoretical solution for T_w at various combinations of the input data as follows: (i) T_a between $-17°$ and 40°C (by an equal increment of 1°C) and $e_s(T_a)$ between 0.01 and 7.2 kPa (by an equal increment of 0.05 kPa), and (ii) elevation from 0 (P_a at sea level = 101.325 kPa) to 4500 m (P_a = 58.5 kPa) in 500-m increments. After excluding results leading to a RH > 100% and RH < 5%, 29 515 remaining combinations were analyzed. For the purpose of a direct comparison, the analytically approximated values of T_w^* were also calculated and plotted against T_w obtained by the numerical analysis (Fig. 3). We found a good agreement between T_w and T_w^*, such that the absolute maximum difference between the numerical and analytical solutions was approximately |1.3|°C. However, in order to further improve the accuracy, a regression of T_w with T_w^* was also derived for both the positive and negative ranges of T_w^* (see the regression equations in Fig. 3 caption). Using this modification, the maximum difference between T_w^* and T_w decreased to less than |0.65|°C.

Prior to the use of the regression equations in Fig. 3, the sign of T_w^* has to be determined; as such, when $T_a <$ 0°C, T_w^* will always be negative. In support of these analyses, the m, n, and q coefficients in Eq. (2), and r and

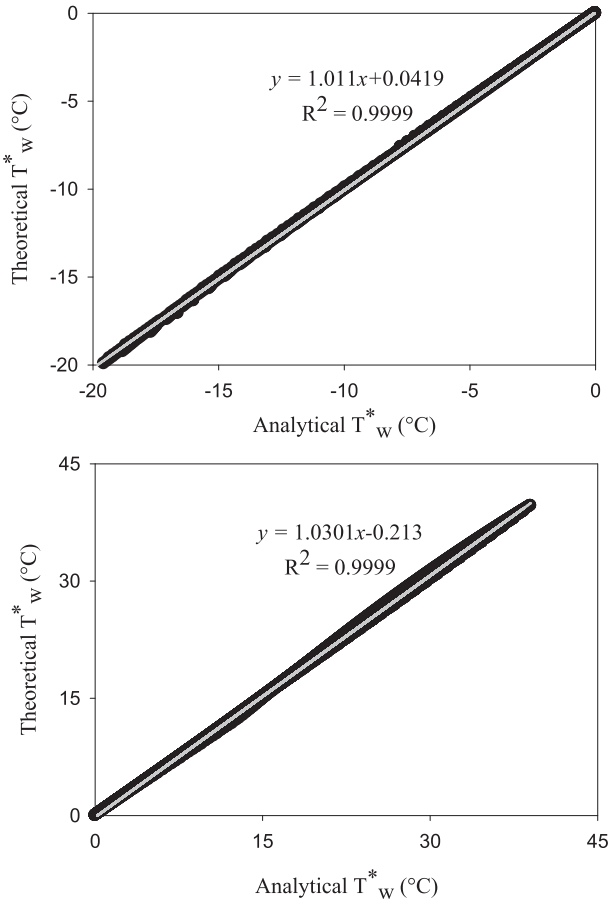

FIG. 3. The quantity T_w^* versus T_w when (a) $T_w^* < 0$°C, $T_w = 1.011(T_w^*) - 0.0419$ with $R^2 = 0.9999$ and (b) $T_w^* \geq 0$°C, $T_w = 1.0301(T_w^*) - 0.213$ with $R^2 = 0.9995$.

s in Eq. (3a), and t and u in Eq. (3b) were statistically estimated and were 100.9254 (for m), 0.155 77 (for n), 0.621 94 (for q), 2 502 535.259 (for r), 2385.764 24 (for s), 2 839 683.144 (for t), and 212.563 84 (for u). Nevertheless, when the T_a is positive ($T_a \geq 0$°C), the positive sign of T_w^* is not guaranteed. For example, assume that the T_a is 2°C, the elevation is $H = 3500$ m, and e_a is 0.16 kPa (RH ≈ 23%); the T_w^* calculated by the iterative solution (Eq. 4) is −4.52°C ($T_a \geq 0$ and $T_w^* < 0$). However, in the same example, if T_a is 14°C, then T_w^* would be 1.6°C ($T_a \geq 0$ and $T_w^* > 0$). To find out whether T_w^* is positive or negative, we define the $F(T)$ function from Eq. (4) as

$$F(T) = a\exp\left(\frac{bT}{T+c}\right) - e_a - \gamma P_a(T_a - T). \quad (13)$$

Notice again that the root of this function represents the T_w^* [$F(T_w^*) = 0$]. Considering the graphical derivation of Figs. 1e–h, T_w^* can only be positive if the root of $F(T)$ falls between $F(0)$ and $F(T_a)$ or in other words, $F(0) \times F(T_a) < 0$. Substituting these values into Eq. (13) yields

$$F(0) = 0.611 - e_a - \gamma P_a T_a, \quad (14a)$$

$$F(T_a) = e_s(T_a) - e_a. \quad (14b)$$

Because RH < 1 and $e_a < e_s(T_a)$, $F(T_a)$ from Eq. (14b) will always be positive. This means that T_w^* will be positive only when $F(0) < 0$ [since $F(0) \times F(T_a)$ is negative], or

$$T_a > \frac{0.611 - e_a}{\gamma P_a}. \quad (15)$$

We further examined the differences between T_w and the modified T_w^* (Fig. 3) as not only a function of T_a but also differences in RH and elevation as well (Fig. 4). Interestingly, when $T_a < 0$°C, the maximum difference was only |0.17|°C. However, when $T_a \geq 0$°C, the difference ranged between ±0.65°C with the largest observed differences (≥|0.5|°C) occurring when conditions were (i) $T_a \geq 39$°C and 31% < RH < 65%, (ii) $T_a \geq 35$°C, 5% < RH < 8%, and when (iii) 27° < T_a < 34°C and RH > 98%. This means that the actual temperature and/or the relative humidity values have to be very high to cause a difference larger than |0.5|°C between the theoretical and the analytical wet-bulb temperature. In general terms, when the T_a increased, the difference between our two compared approaches also increased slightly. The effects of H on $T_w^* - T_w$ were relatively small and its general pattern across the range of T_a and RH remained similar (Fig. 4).

The variation of $T_w^* - T_w$ with H, RH, and T_a was also evaluated (Fig. 5). We found that (i) an elevation change from the sea level to $H = 2000$ m does not significantly affect the difference of $T_w^* - T_w$, although a slight increase was observable (cf. Fig. 5a). For $H > 3000$ m, differences increase at a higher rate when compared to those sea level conditions. These results indicate that larger differences in $T_w^* - T_w$ are expected when $H >$ 3000 m, and (ii) as shown in Fig. 5b, four distinct behaviors are exhibited for the $T_w^* - T_w$ as RH increases. The differences decrease as RH increases from 5% to 20%, increases between 20% < RH < 50%, decreases between 50% < RH < 85%, and finally remain approximately constant as RH varies between 85% and 100%. In addition, the largest differences were apparent when RH is near to 5% or about 50%, and (iii) Fig. 5c demonstrates that the proposed analytical method overestimates T_w (relative to $T_w^* T_w^*$) when 21°C ≤ T_a ≤ 25°C regardless of the value of the RH and H. When $T_a > 8$°C, the range of $T_w^* - T_w$ increased as T_a increases, with the rate being considerably higher when $T_a \geq 26$°C. The two distinct sections in the range of $T_w^* - T_w$ when 0°C < T_a ≤ 8°C result from the fact that positive dry-bulb

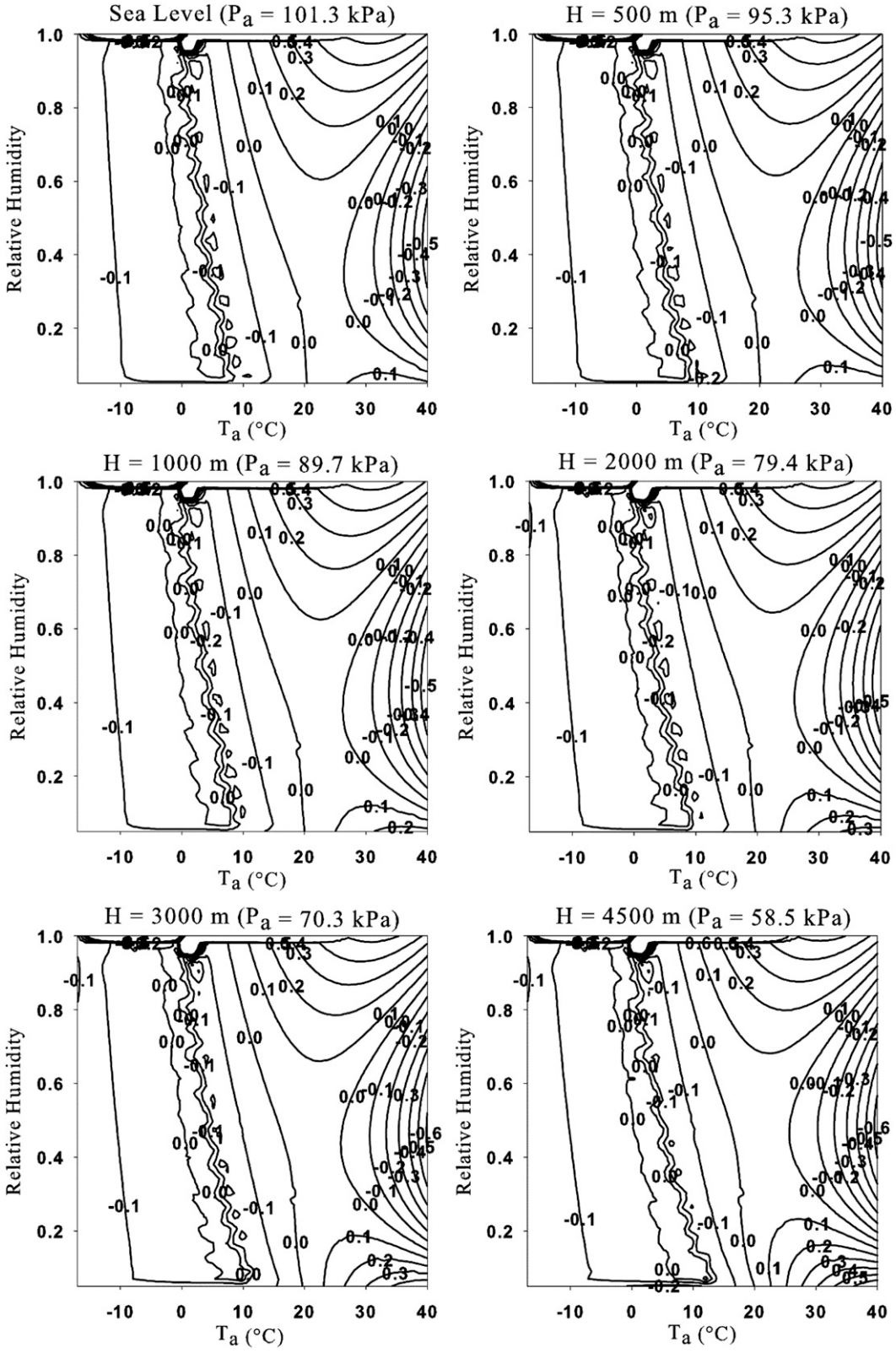

FIG. 4. Difference between T_w Eq. (1) and T_w^* as a function of T_a and RH at elevations ranging from sea level to 4500 m. The y axis is % RH.

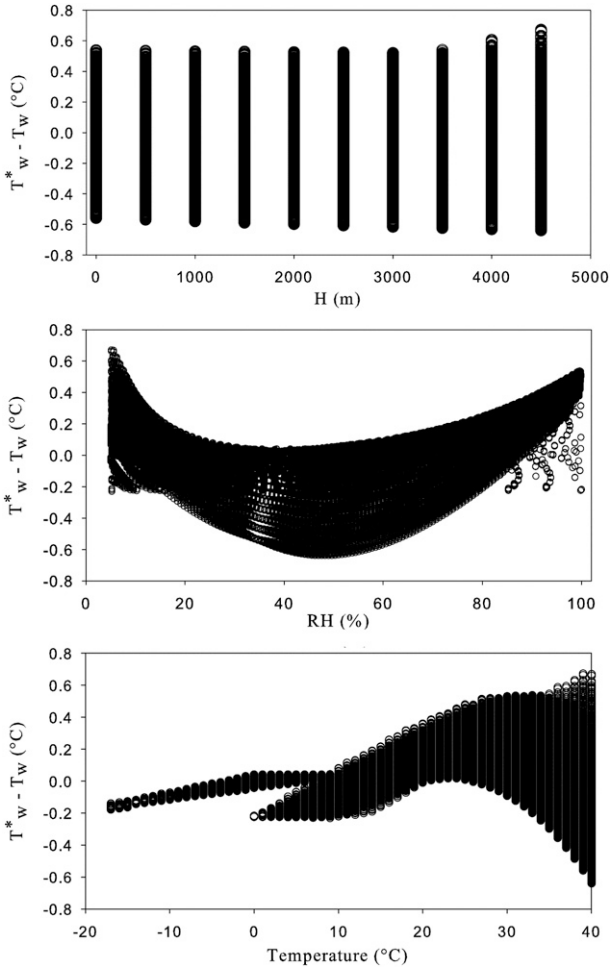

FIG. 5. Variation of $T_w^* - T_w$ versus (top) H, (middle) RH, and (bottom) T_a.

temperatures can provide negative T_w values (i.e., the upper section). Finally, when $T_a < 0$°C, the $T_w^* - T_w$ differences decrease as T_a decreases and both maximum and minimum values of $T_w^* - T_w$ became smaller (Fig. 5c).

The mean absolute error (MAE) and the root-mean-squared errors (RMSE) for the proposed analytical solution were less than 0.15° and 0.2°C, respectively. When T_a was positive, MAE and RMSE were 0.15° and 0.21°C, respectively, but were 0.07° and 0.08°C, respectively, when T_a was <0°C.

4. Conclusions

The wet-bulb temperature is an important psychrometric parameter with implications in environmental, meteorological, and agricultural basic research and applied applications. Historically, the theoretical equation for the T_w has no direct solution, and to find and accurate estimation typically relied upon a trial and error process that requires significant CPU time. On the contrary, the methodology here described, based on second-order polynomial fit, is computationally fast and accurate. In this study, an easy-to-use and accurate analytical solution for calculating the thermodynamic wet-bulb temperature for elevations up to 4500 m above MSL is presented. The reason for this upper bound is because the uncertainty in the psychrometric constant increases to >30% above 4500 m above MSL (Simões-Moreira 1999). Moreover, since the equation for calculating the atmospheric pressure head was used in both methods, we assumed it would not be a significant source of uncertainty and not change the difference between the theoretical and the analytical solutions of T_w. It was found that the wet-bulb temperature for both positive and negative ranges of the air temperature can be simulated by a second-order equation. The suggested technique seems to converge with the other known approach when $-17° \leq T_a < 0$°C, so that the maximum difference in predicting T_w did not exceed |0.17|°C. When $T_a \geq 0$°C, $T_w^* - T_w$ were within ±0.65°C. The larger absolute differences between the observed comparison T_w calculated with T_a in the positive range contrasted with the negative range was likely due to two major reasons: (i) the positive values spanned a larger range and (ii) the relationship between wet-bulb temperature and T_a is more curvilinear when $T_a \geq 0$°C. Therefore, the comparative use of the three environmental conditions leads to larger uncertainties in estimating the second-order polynomial coefficients (i.e., λ, φ, and ψ). This study also proved again that values of 5.68×10^{-4} to 6.42×10^{-4} when $T_w < 0°$ and $0° \leq T_w \leq 30$°C converged with other estimates of the thermodynamic psychrometric constant. The proposed method can provide more detailed understanding of hydrostatic properties of air containing water vapor, particularly in the estimation of the wet-bulb temperature without the use of alternative and computationally cumbersome iterative approaches.

Acknowledgments. The authors wish to thank Prof. R. Stull for his response to our inquiry, and also Dr. Th. Bellinger for suggesting useful references that greatly improved the quality of this work. HWL wishes to thank the National Science Foundation under the Grant EF-102980. Any opinions, findings, and conclusions or recommendations expressed in this material are those of the authors and do not necessarily reflect the views of the National Science Foundation. The authors are thankful for the thoughtful comments from three anonymous reviewers.

REFERENCES

Alves, I., J. C. Fontes, and L. S. Pereira, 2000: Evapotranspiration estimation from infrared surface temperature. II: The surface

temperature as a wet bulb temperature. *Trans. ASAE,* **43,** 591–598.

Angström, A., 1920: Studies of the frost problem I. *Geogr. Ann.,* **2,** 2–32.

ASABE, 2006: ASABE standards: Psychrometric data. American Society of Agriculture and Biological Engineers ASAE D271.2 APR1979 (R2005), 27 pp. [Available online at http://elibrary.asabe.org/standards.asp.]

ASHRAE, 1997: *1997 ASHRAE Handbook: Fundamentals.* SI ed. ASHRAE, 1426 pp.

Balogun, A. A., O. O. Jegede, T. Foken, and J. O. Olaleye, 2002a: Comparison of two Bowen-ratio methods for the estimation of sensible and latent heat fluxes at Ile-Ife, Nigeria. *J. Afr. Meteor. Soc.,* **5** (2), 63–69.

——, ——, ——, and ——, 2002b: Estimation of sensible and latent heat fluxes over bare soil using bowen ratio energy balance method at a humid tropical site. *J. Afr. Meteor. Soc.,* **5** (1), 63–71.

Brooker, D. B., 1967: Mathematical model of the psychrometric chart. *Trans. ASAE.,* **10,** 558–560.

Buck, A. L., 1981: New equations for computing vapor pressure and enhancement factor. *J. Appl. Meteor.,* **20,** 1527–1532.

Campbell, G. S., and J. M. Norman, 1998: *An Introduction to Environmental Biophysics.* 2nd ed. Springer-Verlag, 286 pp.

Chappell, C. F., E. L. Magaziner, and J. M. Fritsch, 1974: On the computation of isobaric wet-bulb temperature and saturation temperature over ice. *J. Appl. Meteor.,* **13,** 726–728.

Chau, K. V., 1980: Some new empirical equations for properties of moist air. *Trans. ASAE,* **23,** 1266–1271.

Dunin, F. X., and E. A. N. Greenwood, 1986: Evaluation of the ventilated chamber for measuring evaporation from a forest. *Hydrol. Processes,* **1,** 47–62.

Gan, G., and S. B. Riffat, 1999: Numerical simulation of closed wet cooling towers for chilled ceiling systems. *Appl. Therm. Eng.,* **19,** 1279–1296.

Loescher, H. W., B. E. Law, L. Mahrt, D. Y. Hollinger, J. L. Campbell, and S. C. Wofsy, 2006: Uncertainties in, and interpretation of, carbon flux estimates using the eddy covariance technique. *J. Geophys. Res.,* **111,** D21S90, doi:10.1029/2005JD006932.

——, C. V. Hanson, and T. W. Ocheltree, 2009: The psychrometric constant is not constant: A novel approach to enhance the accuracy and precision of latent energy fluxes through automated water vapor calibrations. *J. Hydrometeor.,* **10,** 1271–1284.

Monteith, J. L., 1965: Evaporation and environment. *Proceedings of the 19th Symposium of the Society for Experimental Biology,* Cambridge University Press, 205–234.

Murray, F. W., 1967: On the computation of saturation vapor pressure. *J. Appl. Meteor.,* **6,** 203–204.

Schmidt, J. L., and P. J. Waite, 1962: Summaries of wet-bulb temperature and wet-bulb depression for grain drier design. *Trans. ASAE,* **5,** 186–189.

Schurer, K., 1981: Confirmation of a lower psychrometer constant. *J. Phys.,* **14E,** 1153.

Simões-Moreira, J. R., 1999: A thermodynamic formulation of the psychrometer constant. *Meas. Sci. Technol.,* **10,** 302–311.

Slatyer, R. O., and I. C. McIlroy, 1961: *Practical Microclimatology.* UNESCO, 297 pp.

Smith, J. W., 1920: Predicting minimum temperatures from the previous afternoon wet-bulb temperature. *Mon. Wea. Rev.,* **48,** 640–641.

Sreekanth, S., H. S. Ramaswamy, and S. Sablani, 1998: Prediction of psychrometric parameters using neural networks. *Drying Technol.,* **16,** 825–837.

Stull, R., 2000: *Meteorology for Scientists and Engineers.* 3rd ed. Discount Textbooks, 924 pp.

——, 2011: Wet-bulb temperature from relative humidity and air temperature. *J. Appl. Meteor. Climatol.,* **50,** 2267–2269.

Tejeda-Martínez, A., 1994: On the evaluation of the wet bulb temperature as a function of dry bulb temperature and relative humidity. *Atmósfera,* **7,** 179–184.

Wai, M.-K., and E. A. Smith, 1998: Linking boundary layer circulations and surface processes during FIFE 89. Part II: Maintenance of secondary circulation. *J. Atmos. Sci.,* **55,** 1260–1276.

Wexler, A., 1976: Vapor pressure formulation for water in range 0 to 100°C. A revision. *J. Res. Natl. Bur. Stand.,* **80,** 775–785.